

## Decoherence by a chaotic many-spin bath

J. Lages,<sup>1</sup> V. V. Dobrovitski,<sup>1</sup> M. I. Katsnelson,<sup>2</sup> H. A. De Raedt,<sup>3</sup> and B. N. Harmon<sup>1</sup>

<sup>1</sup>*Ames Laboratory and Department of Physics and Astronomy, Iowa State University, Ames, Iowa 50011, USA*

<sup>2</sup>*Institute for Molecules and Materials, Radboud University Nijmegen, Toernooiveld 1, 6525 ED Nijmegen, The Netherlands*

<sup>3</sup>*Department of Applied Physics, Materials Science Centre, University of Groningen, Nijenborgh 4, NL-9747 AG Groningen, The Netherlands*

(Received 10 May 2004; revised manuscript received 9 March 2005; published 31 August 2005)

We numerically investigate decoherence of a two-spin system (central system) by a bath of many spins  $1/2$ . By carefully adjusting parameters, the dynamical regime of the bath has been varied from quantum chaos to regular, while all other dynamical characteristics have been kept practically intact. We explicitly demonstrate that for a many-body quantum bath, the onset of quantum chaos leads to significantly faster and stronger decoherence compared to an equivalent nonchaotic bath. Moreover, the nondiagonal elements of the system's density matrix, the linear entropy, and the fidelity of the central system decay differently for chaotic and nonchaotic baths. Therefore, knowledge of the basic parameters of the bath (strength of the system-bath interaction, and the bath's spectral density of states) is not always sufficient, and much finer details of the bath's dynamics can strongly affect the decoherence process.

DOI: [10.1103/PhysRevE.72.026225](https://doi.org/10.1103/PhysRevE.72.026225)

PACS number(s): 05.45.Pq, 03.65.Yz, 75.10.Nr, 03.67.-a

### INTRODUCTION

Real physical systems are never isolated. Interaction of a quantum system with its environment leads to decoherence: the initial pure state of the system quickly decays into an incoherent mixture of several states [1]. Modern experiments provide much information about the decoherence dynamics of single (or few) ions [2], Cooper pairs [3], or spins [4], and require a comprehensive theory for adequate understanding. Decoherence is also a major obstacle to building a practical quantum computer [5]. Interaction of a quantum computer with the bath leads to a fast generation of errors, and an accurate theory is needed to find a way of controlling this process.

Decoherence is a complex quantum many-body phenomenon, and its detailed description is a challenging problem. Many theoretical approaches eliminate the environment from consideration, approximating its influence by suitably chosen operators (deterministic or stochastic), and retaining only basic information: the strength of the system-bath interaction, characteristic energies or times of the bath, etc. [6]. Such methods often work well, but many situations require detailed account of the bath's internal dynamics. Recently, the role of quantum chaos [7] in the decoherence process has become a subject of debate [8–10]. One line of argument suggests that the chaotic bath (i.e., the bath having only a few trivial integrals of motion) is “a stronger decoherer” [8] than an integrable bath (i.e., the bath possessing a complete set of the integrals of motion). Within this line of argument, the central system is replaced by a static perturbation acting on the bath; in general, the semiclassical trajectories of the chaotic bath diverge exponentially under such a perturbation, with the rate governed by the Lyapunov's exponents of the bath, while for the regular bath the divergence is slower. However, other regimes of the bath's dynamics are also possible, and the decoherence rate depends on the specific dynamical regime. For example, when the system-bath interaction becomes extremely small, so that the perturbation theory

is applicable, it appears that the regular bath leads to faster decoherence than the chaotic one [9]. So far, many dynamical regimes of the chaotic vs. regular baths have been studied [10], and many valuable insights about the decoherence have been obtained. However, the basic approach, i.e., replacement of the actual central system by a static perturbation acting on a bath, is valid only in the simplest cases. Even in slightly more complex situations, it appears that the answer strongly depends on particular choice of the perturbation operator [11]. Moreover, the majority of relevant work [10] treats the bath semiclassically, as a particle (or a single large spin) with an integrable or a chaotic Hamiltonian.

Therefore, an important question remains unanswered: is the onset of quantum chaos important for the real-world situation when both the system and the bath are fundamentally quantum many-body objects with nontrivial dynamics? In this paper, we give an affirmative answer to this question. In contrast with previous work, we do not replace the system or the bath by a static perturbation (in fact, for our model such replacement is impossible, see below). We go beyond the semiclassical one-body description, realistically considering the spin environment as many interacting spins  $1/2$ , which have no well-defined semiclassical limit. It is surprising and interesting that even in the absence of the semiclassical analog for our bath, the results we obtain agree with the conclusions drawn based on qualitative semiclassical consideration. For the case when the system-bath interaction is not extremely small (i.e., for the nonperturbative regime), we show that the chaotic bath decoheres the central system stronger and faster than an equivalent nonchaotic one, and changes the dynamics of the decay of nondiagonal elements of the system's density matrix.

The bath of spins  $1/2$  (nuclear or electron spins, magnetic impurities) constitutes a major source of decoherence for nuclear magnetic resonance (NMR) experiments, decoherence of phosphorus spins in Si [12], spins in magnetic molecules [13] and quantum dots [14]. Two-level defects, governing decoherence in Josephson junctions [15], can also be

modeled as spins 1/2. Even small coupling between the bath spins can make the bath chaotic (see below), and it is important to understand how this affects the decoherence process.

The rest of the paper is organized as follows. In Sec. I, we describe the model and discuss how, by changing the parameters, the bath's dynamics can be smoothly varied from chaotic to regular. We also present qualitative discussion of the influence of quantum chaos on the decoherence process. Section II presents general features of the evolution of the central system and discusses two stages of decoherence. In Sec. III, we consider the first stage of decoherence, the decay of the short-time oscillations, and demonstrate how the temporal evolution of the central system is affected by the onset of quantum chaos in the bath. Section IV is devoted to the study of the impact of chaos on the long-time evolution of the system and on the pointer states of the system. In Sec. V, we summarize our results.

### I. CENTRAL SYSTEM–BATH INTERACTION MODEL

The dynamics of a system decohered by the spin bath is affected by many factors. In order to conclusively separate the impact of chaos in the bath, and to provide the knowledge needed for more complex studies, we need a simple, well-characterized, but realistic model. Here, we consider a central system made of two isotropically coupled spins 1/2,  $\mathbf{S}_1$  and  $\mathbf{S}_2$ , where the spin  $\mathbf{S}_1$  interacts with an environment made of a large number of spins 1/2  $\mathbf{I}_k$ , so the Hamiltonian describing the compound system (the two central spins plus the bath) is

$$H = JS_1 \cdot S_2 + S_1 \cdot \sum_k A_k \mathbf{I}_k + H_B, \quad (1)$$

where  $A_k$  are the system-bath coupling constants, and  $H_B$  is the Hamiltonian of the bath. Such models as Eq. (1) are often encountered in the description of the cross relaxation and double resonance in nuclear magnetic resonance [16], and were recently used to study destruction of the Kondo effect by decoherence [17].

It is important to note here that both the central system's Hamiltonian and the system-bath interaction term in Eq. (1) are rotationally symmetric. Thus the central system in principle cannot be replaced by a perturbation, whether static or dynamic. Such a perturbation, if it were possible, should be linear in spin operators  $\mathbf{I}_k$ , i.e., it should have a form  $\mathbf{H}_k \cdot \mathbf{I}_k$ , which would break the original rotation symmetry of the system-bath interaction. Crudely speaking, the fields  $\mathbf{H}_k$  can not be directed anywhere because the system-bath coupling has no preferred direction.

Furthermore, for a conclusive study, we need a simple, well characterized but realistic many-spin model for the spin bath, which would allow changing the bath dynamical regime from chaotic to regular without strongly affecting other properties of the bath. A good candidate satisfying these conditions is the "spin glass shard" model [18] with the Hamiltonian

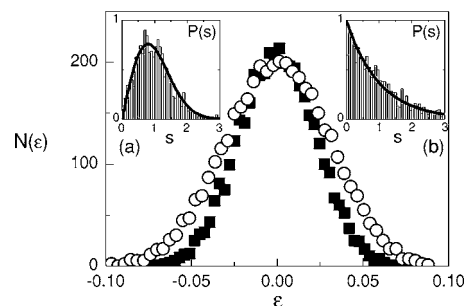


FIG. 1. The spectral densities of states  $N(\epsilon)$  vs energy  $\epsilon$  for regular bath (■) with  $\Gamma_0=0.008$ , and for chaotic bath (○) with  $\Gamma_0=0.04$ . All other parameters are the same, and  $h_0=0.014$ . Insets (a) and (b) show the level spacing distributions  $P(s)$  for chaotic and regular baths, respectively. The thick lines show the orthogonal Wigner-Dyson and Poisson distributions for chaotic and nonchaotic baths, respectively.

$$H_B = \sum_{k,l} \Gamma_{kl} I_k^x I_l^x + \sum_k h_k^z I_k^z + \sum_k h_k^x I_k^x \quad (2)$$

with random  $\Gamma_{kl}$  and  $h_k^{x,z}$ , uniformly distributed in the intervals  $[-\Gamma_0, \Gamma_0]$  and  $[0, h_0]$ , respectively; the bath spins  $I_k$  are placed on a two-dimensional square lattice, and only nearest neighbors  $k$  and  $l$  are coupled with the strength  $\Gamma_{kl}$ . This model describes the regular-to-chaotic transition in a simple and clear way, and permits straightforward control of the bath's dynamics [18]. For small  $\Gamma_0$ , the bath is integrable, and becomes chaotic for  $\Gamma_0 > \Gamma_{cr} = C_1 h_0 / (zN)$ , where  $C_1$  is some numerical coefficient (which can be as large as 32),  $N$  is the number of bath spins and  $z$  is the number of neighbors coupled via the term  $\Gamma_{kl} I_k^x I_l^x$ . In real baths with  $N \sim 10^6$  or more, the onset of chaos becomes relevant already for couplings  $\Gamma_{kl}$  which are extremely small in comparison with  $h_0$ . However, the onset of chaos very weakly affects the large-scale spectral properties of the bath, such as the spectral density of states, which are governed almost completely by the fields  $h_k^{x,z}$ . For example, the width of the spectrum  $W$  can be estimated as  $W^2 = (1/16)[\sum \Gamma_{kl}^2] + (1/4)[\sum (h_k^z)^2 + (h_k^x)^2]$ , so that the contribution from the couplings  $\Gamma_{kl} I_k^x I_l^x$  is negligible for realistic baths with very large  $N$ . In fact, due to the small prefactor, the contribution of  $\Gamma_{kl}$  is small already for  $N = 12-16$ . We verified these bath properties by direct diagonalization of the Hamiltonian (2), keeping the value of  $h_0$  constant and varying  $\Gamma_0$ . Calculation of the level spacing statistics  $P(s)$  [7] [insets (a),(b) in Fig. 1] clearly shows that  $P(s)$  changes from the orthogonal Wigner-Dyson form for a chaotic bath to the Poisson form for a regular bath. At the same time, the spectral density of states is affected very weakly, even for  $N=12$ : the width of the spectrum changes from  $W=0.048$  for regular bath to  $W=0.060$  for the chaotic bath.

#### A. Static central system: Semiclassical consideration

Our goal is to understand how the onset of chaos in the bath affects the decoherence process. Let us first recall the basic ideas of decoherence and understand qualitatively the

role of the bath's internal dynamics, following Ref. [8]. For simplicity, let us consider a static central system coupled to a bath, so that the Hamiltonian of the compound system (central system plus the bath) is  $H=gQ \otimes P + \mathbf{1} \otimes H_B$ , where  $Q$  and  $P$  are the operators acting on the system and the bath, respectively,  $g$  is the coupling strength, and  $H_B$  is the bath's internal Hamiltonian, which determines whether the bath is chaotic or regular. Initially, the central system is in a superposition of the states  $|q_1\rangle$  and  $|q_2\rangle$  such that  $Q|q_1\rangle=q_1|q_1\rangle$  and  $Q|q_2\rangle=q_2|q_2\rangle$ , and the bath is in a state  $|\chi_0\rangle$ . The time-dependent wave function of the compound system is

$$|\Psi(t)\rangle = |q_1\rangle \otimes |\chi_1(t)\rangle + |q_2\rangle \otimes |\chi_2(t)\rangle, \quad (3)$$

where  $|\chi_1(t)\rangle = \exp(-iH_B t - igq_1 P t)|\chi_0\rangle$ , and  $|\chi_2(t)\rangle = \exp(-iH_B t - igq_2 P t)|\chi_0\rangle$ . The state of the system is characterized by the reduced density matrix  $\rho = \text{Tr}_B |\Psi(t)\rangle\langle\Psi(t)|$ , and, in particular, by the off-diagonal element of the density matrix  $\rho_{12} = \langle q_1 | \rho | q_2 \rangle$ . Due to the system-bath coupling, the correlations are established between the system and the bath, and the off-diagonal element  $\rho_{12} \propto \langle \chi_1(t) | \chi_2(t) \rangle$  is determined by the bath's dynamics. Initially,  $|\chi_1\rangle = |\chi_2\rangle = |\chi_0\rangle$ , but in the course of the evolution, the difference develops between the states  $|\chi_1\rangle$  and  $|\chi_2\rangle$ , the overlap between these states becomes smaller, so the value of  $\rho_{12}$  decreases. At long times, when  $\rho_{12} \approx 0$ , the initial superposition of the system's states becomes an incoherent mixture of  $|q_1\rangle$  and  $|q_2\rangle$ .

The decay rate of the overlap  $\langle \chi_1(t) | \chi_2(t) \rangle$  (and therefore the decoherence rate) is strongly affected by the bath's internal dynamics. The time evolution of the absolute value of the overlap

$$O(t) = |\langle \chi_1(t) | \chi_2(t) \rangle|^2 = |\langle \chi_0 | \exp(-iH_1 t) \exp(iH_2 t + iV t) | \chi_0 \rangle|^2, \quad (4)$$

where  $V = g(q_2 - q_1)P$ , is a well-known problem in the quantum chaos theory. The quantity  $O(t)$  is called the Loschmidt echo (LE), and describes the system's reaction to the small perturbation of the Hamiltonian, the evolution of the overlap of two wave packets  $|\chi_1\rangle$  and  $|\chi_2\rangle$  subjected to slightly different Hamiltonians. If such wave packets are considered quasiclassically then their positions are determined by the classical equations of motion, and the distance between two classical trajectories in a chaotic system diverge exponentially with the rate determined by the maximal Lyapunov's exponent. Therefore, one may guess that  $O(t)$  decreases exponentially with time for chaotic systems, and subexponentially for regular systems. Correspondingly, the decoherence is probably faster for a chaotic bath than for a regular one.

### B. Validity of semiclassical consideration

This semiclassical argument has many deficiencies. For instance, criticism has focused on the simplified treatment of the Loschmidt echo: the exponential decay determined by the Lyapunov's exponent (the Lyapunov's regime) is only one of many other possible regimes of LE decay [10]. For very weak system-bath coupling, i.e., for very small perturbation  $V$ , the Loschmidt echo decay can be investigated using perturbation theory, and the results can be generalized to

include many cases of the decoherence of a system by a chaotic vs regular bath. Such a perturbative approach gives exactly the opposite result: the chaotic bath is a less efficient "decoherer" than the regular bath. The perturbative arguments are easy to understand qualitatively: the decoherence is determined primarily by the low-energy bath excitations, and for chaotic baths, due to the level repulsion, the density of the low-energy excitations is much smaller than for the regular baths [because the Wigner-Dyson distribution  $P_{WD}(s)$  of the level splittings  $s$  goes to zero for  $s \rightarrow 0$ , i.e., the number of the low-energy excitations in a chaotic bath goes to zero, while the Poisson distribution  $P_P(s)$  describing the regular baths gives a finite number of low-energy excitations,  $P_P(s) = 1$  at  $s = 0$ ].

The simplified treatment of the LE decay is not the only drawback of the semiclassical argument above. First, the decoherence is quantified not only by its rate but also by its "strength," i.e., by the question of how strongly the final states of the decohered system (the so-called pointer states; see the more detailed discussion in Sec. II) differ from the eigenstates of the system's Hamiltonian. The influence of chaos has not been studied in this context yet. Second, close examination reveals much more serious problems with the semiclassical argument. (i) Realistic central systems are rarely static [e.g., in Eq. (1) the central system has a nonzero internal Hamiltonian  $\mathcal{J}\mathbf{S}_1 \cdot \mathbf{S}_2$ ], so the perturbation  $V$  is usually time-dependent. (ii) The LE decay is, in general, not universal, and depends on the specific form of the perturbation  $V$ , so that by choosing different operators  $P$  and  $Q$ , one can arrive at mutually exclusive conclusions [11]. (iii) The semiclassical consideration is inapplicable to a large class of baths made of spins 1/2, which do not have a well-defined semiclassical limit, and interpretation of their motion in terms of wavepackets is inapplicable. (iv) And, most importantly, for majority of realistic systems, the decoherence problem can not be reduced in principle to the LE decay: e.g., the system-bath coupling described by Eq. (1) [see also the discussion following Eq. (1)] cannot be cast in the form  $Q \otimes P$ .

Therefore, in order to understand decoherence in realistic systems, we should go beyond the semiclassical LE decay considerations (but keep in mind their great heuristic value), and beyond the perturbative treatment (which is valid only for extremely weak system-bath couplings). Detailed studies satisfying these conditions and considering realistic many-spin baths, have not been previously pursued, but the present work provides such a study. We show that in spite of their formal inapplicability to the bath of many spins 1/2, the semiclassical considerations grasp many essential physical details of the decoherence process.

## II. TIME EVOLUTION OF THE CENTRAL SYSTEM: GENERAL PICTURE

We assume that initially, at  $t=0$ , the central system is in singlet state

$$|\psi_0\rangle = (|\uparrow\downarrow\rangle - |\downarrow\uparrow\rangle)/\sqrt{2} \quad (5)$$

and is uncorrelated with the bath. This singlet state is maximally entangled, and the knowledge of the state of one of the



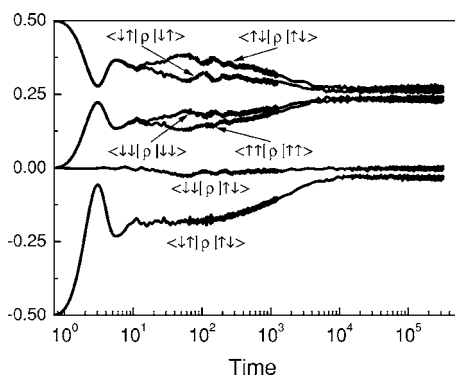


FIG. 2. Time evolution of the elements of the central system's reduced density matrix  $\rho$  for a bath with  $\Gamma_0=0.04$  and  $h_0=0.014$ . The dynamics of the diagonal elements  $\langle \uparrow\uparrow|\rho|\uparrow\uparrow \rangle$ ,  $\langle \downarrow\downarrow|\rho|\downarrow\downarrow \rangle$ ,  $\langle \downarrow\uparrow|\rho|\uparrow\uparrow \rangle$ ,  $\langle \uparrow\downarrow|\rho|\uparrow\downarrow \rangle$ , and of the off-diagonal elements  $\text{Re}\langle \uparrow\downarrow|\rho|\uparrow\downarrow \rangle$ ,  $\text{Re}\langle \downarrow\uparrow|\rho|\uparrow\downarrow \rangle$  is shown. The coupling energy between the two central spins is  $J=0.1$  and the coupling between the bath and the central system is characterized by  $b=1.37$  (also see text). The energy and time quantities are dimensionless.

spins gives us directly the state of the other. We also assume that the initial state of the bath  $|\chi_0\rangle$  is a superposition of all basis states with random coefficients. This assumption is valid for a general bath of nuclear spins at temperatures above few tenths of Kelvin, which is the case for the majority of realistic and experimentally interesting situations. We study decoherence by numerically solving the time-dependent Schrödinger equation for the wave function  $|\Psi(t)\rangle$  of the compound system (the two central spins plus the bath), using the Hamiltonians (1) and (2). We use Chebyshev's polynomial expansion of the evolution operator, in order to work with large Hilbert spaces and to study the system's dynamics at extremely long times [19,20]. The validity of the very long-time simulations used in this paper is guaranteed by the Chebyshev polynomial expansion method, provided that a sufficiently large number of the terms is included into the evolution operator. Moreover, we checked the validity of the simulations directly, using standard methods: (i) comparison with the exactly solvable models, and (ii) comparison of different simulations with different tolerance parameters. We have studied the baths with up to  $N=16$  spins; our studies show that the evolution of the reduced density matrix elements do not change much already for  $N>10$ . Most of the results presented below are obtained for  $N=12$ , and the computationally extensive simulations with  $N=16$  were used to check the most important statements. A wide range of the parameters  $J$ ,  $h_0$ ,  $\Gamma_0$ ,  $N$ , and different sets  $\{A_k\}_{k=1,N}$  have been explored, and the rest of the paper presents typical results. In the remainder of the paper, energy and time are dimensionless quantities.

At  $t=0$ , the reduced density matrix of the central system  $\rho$  describes a pure state, and the only nonzero entries are the diagonal elements  $\langle \uparrow\downarrow|\rho|\uparrow\downarrow \rangle = \langle \downarrow\uparrow|\rho|\downarrow\uparrow \rangle = 1/2$ , and the off-diagonal elements  $\langle \downarrow\uparrow|\rho|\uparrow\downarrow \rangle = \langle \uparrow\downarrow|\rho|\downarrow\uparrow \rangle = -1/2$ . Due to the system-bath interaction the elements of the reduced density matrix  $\rho$  change with time. Their typical evolution is shown in Fig. 2. Two stages are clearly seen. At first, the bath rap-

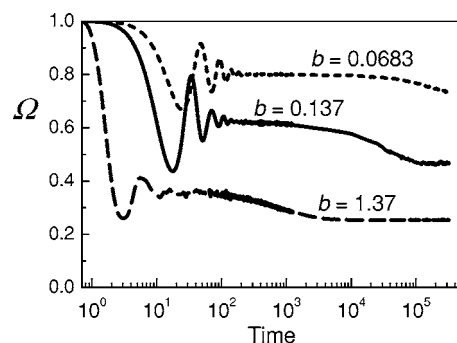


FIG. 3. Time evolution of the central system's linear entropy  $\Omega$  for different values of the central system-bath coupling  $b=1.37$  (dashed line),  $0.137$  (solid line), and  $0.0683$  (dotted line). The parameters of the bath's Hamiltonian are the same as in Fig. 2:  $\Gamma_0=0.04$ ,  $h_0=0.014$ , and the coupling between the two central spins is  $J=0.1$ .

idly decoheres the central system, and the system's state becomes mixed. The initial perfect correlation between the states  $|\downarrow\uparrow\rangle$  and  $|\uparrow\downarrow\rangle$  is gradually destroyed, so that the off-diagonal element  $\langle \downarrow\uparrow|\rho|\uparrow\downarrow \rangle$  rapidly oscillates and decays towards zero. Decoherence is accompanied by excitation of the system's triplet states (including the initially absent  $|\uparrow\uparrow\rangle$  and  $|\downarrow\downarrow\rangle$  states). As a result, all the elements of  $\rho$  oscillate, mirroring the quantum oscillations of the central system between the singlet and triplet. At the second stage, much later (note the logarithmic scale of the time axis), thermalization of the system takes place at much slower rate. In the example shown in Fig. 2, the system-bath coupling is strong enough to almost completely destroy the entanglement between the central spins (the off-diagonal element  $\langle \downarrow\uparrow|\rho|\uparrow\downarrow \rangle$  is almost zero at  $t\rightarrow\infty$ ), and to almost equally populate all levels of the system so that  $\langle \uparrow\uparrow|\rho|\uparrow\uparrow \rangle \approx \langle \downarrow\downarrow|\rho|\downarrow\downarrow \rangle \approx \langle \downarrow\uparrow|\rho|\uparrow\downarrow \rangle \approx \langle \uparrow\downarrow|\rho|\downarrow\uparrow \rangle \approx 1/4$  at  $t\rightarrow\infty$ . Throughout the whole system's evolution the other off-diagonal elements of the reduced density matrix remain close to zero (e.g., see the element  $\langle \downarrow\downarrow|\rho|\uparrow\downarrow \rangle$  in Fig. 2).

The loss of the purity of the system's state can be characterized by the decay of the linear entropy of the central system,  $\Omega = \text{Tr} \rho^2$ . If the central system is in a pure state, the reduced density matrix  $\rho$  is idempotent ( $\rho^2 = \rho$ ), and  $\Omega = 1$ , while for the mixed state  $\Omega < 1$ . The time evolution of  $\Omega$  is shown in Fig. 3. Again, two stages are clearly seen: decaying oscillations at  $0 < t < 300$  followed by an approach to saturation at a much slower rate for  $t > 300$ . Time evolution of  $\Omega$  is shown for three baths, with different strength of the coupling to the central system. As will be shown below, the coupling can be characterized by the quantity

$$b = \sqrt{\sum_{k=1}^N A_k^2}. \quad (6)$$

The decoherence rate increases with  $b$ , and  $\Omega$  saturates at smaller times for larger  $b$ . Also, the saturation value of  $\Omega$  at  $t\rightarrow\infty$  is smaller for larger  $b$  (the central system is more mixed for stronger system-bath coupling). The minimum

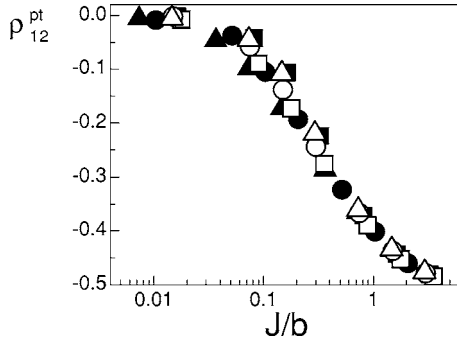


FIG. 4. Pointer state value  $\rho_{12}^{pt}$  of the off-diagonal reduced density matrix element  $\rho_{12}$  as a function of the ratio  $J/b$  for  $h_0=1/\sqrt{2}$  and  $\Gamma_0=0.008$ . The results are presented for different sizes  $N$  of the bath and different system-bath coupling parameters  $b$ :  $N=8$ ,  $b=0.518$  ( $\square$ ),  $N=10$ ,  $b=0.562$  ( $\circ$ ),  $N=12$ ,  $b=0.683$  ( $\triangle$ ),  $N=12$ ,  $b=0.608$  ( $\blacksquare$ ),  $N=12$ ,  $b=0.965$  ( $\bullet$ ), and  $N=12$ ,  $b=1.365$  (25B4). All points fall in the vicinity of a same curve.

value of  $\Omega$  for the system of two spins  $1/2$  is 0.25; this value is achieved at  $t \rightarrow \infty$  for  $b=1.37$ .

Different initial states of the system are differently affected by decoherence, and the states which are affected the least survive the interaction with the bath longer than all others. Thus, at  $t \rightarrow \infty$  any initial state of the system will decay into a mixture of such least-affected states, which are called the pointer states. For the two-spin central system considered here, the pointer states are easy to identify by considering the value of the off-diagonal density matrix element  $\langle \downarrow \uparrow | \rho | \uparrow \downarrow \rangle$ , whose initial value is  $-1/2$ . This matrix element will be of special importance for the rest of the paper, so we introduce a special notation for its real part:  $\rho_{12} = \text{Re} \langle \downarrow \uparrow | \rho | \uparrow \downarrow \rangle$ . The system-bath interaction term  $\mathbf{S}_1 \cdot \sum A_k \mathbf{I}_k$  in Eq. (1) entangles the spin  $\mathbf{S}_1$  with the bath thus destroying the quantum correlations between  $\mathbf{S}_1$  and  $\mathbf{S}_2$ . If the system-bath coupling is strong these correlations are destroyed completely, so that the pointer states of the central system are the product states  $|\uparrow \downarrow\rangle$  and  $|\downarrow \uparrow\rangle$ , with  $\rho_{12}=0$ . However, the internal Hamiltonian of the central system  $J\mathbf{S}_1 \cdot \mathbf{S}_2$  preserves the initial singlet correlation between  $\mathbf{S}_1$  and  $\mathbf{S}_2$ , thus steering the value of  $\rho_{12}$  towards  $-1/2$  (for weak interaction between the system and the bath, the pointer states of the system are the eigenstates of the system's internal Hamiltonian [21], i.e., the initial singlet will be the pointer state). Competition between the two tendencies determines the pointer-state value of  $\rho_{12}$  as  $t \rightarrow \infty$ .

To make these considerations quantitative, we note that the strength of the system's internal coupling is determined by  $J$ . How should we quantify the system-bath interaction? Here we show that the relevant quantity is  $b = \sqrt{\sum_{k=1}^N A_k^2}$ . Figure 4 shows the pointer-state value  $\rho_{12}^{pt}$  of  $\rho_{12}$  obtained from simulations with different sizes of the bath and different values of  $b$  (with the bath parameters kept intact). As one can see, all the results fall on the same master curve, i.e., for fixed internal parameters of the bath  $\Gamma_0$  and  $h_0$ , the value  $\rho_{12}^{pt}$  is determined only by the single ratio  $J/b$ . Figure 4 supports the qualitative arguments given in the previous paragraph: for  $J/b \ll 1$  (strong system-bath coupling)  $\rho_{12}^{pt}=0$ , and for

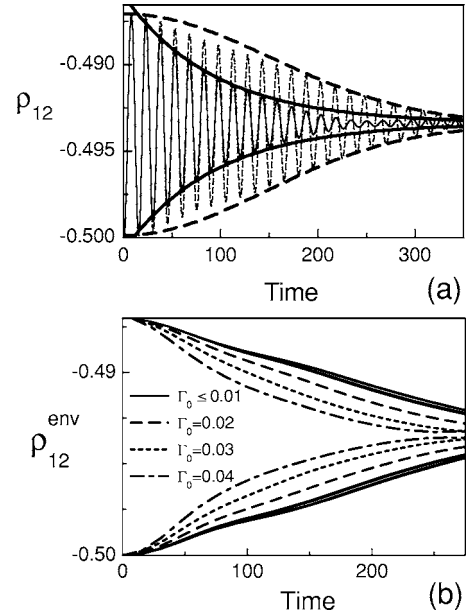


FIG. 5. (a) Short-time evolution of the off-diagonal element  $\rho_{12}(t)$  for chaotic bath  $\Gamma_0=0.04$  (solid curve) and for regular bath  $\Gamma_0=0.008$  (dashed curve). All other parameters of the Hamiltonians (1) and (2) are kept constant, including the individual values of  $A_k$ ,  $h_k$ . (b) Envelopes  $\rho_{12}^{env}$  for regular baths with  $\Gamma_0=0, 0.004, 0.008$ , and  $0.01$  (solid lines, all four outermost curves almost merge with each other) and for chaotic baths with  $\Gamma_0=0.02$  (dash line),  $0.03$  (dot line), and  $0.04$  (dot-dash line). All other parameters of the Hamiltonians (1) and (2) are kept constant, including the individual values of  $A_k, h_k$ . For both panels,  $h_0=0.014$ ,  $J=0.4$ , and  $b=0.0683$ .

$J/b \gg 1$  (weak system-bath coupling)  $\rho_{12}^{pt} = -1/2$ . Therefore, the curve  $\rho_{12}^{pt}(J/b)$  provides direct information about the strength of decoherence.

### III. CHAOTIC VS REGULAR BATH DECOHERENCE: DECAY OF THE OSCILLATIONS AT SHORT TIMES

#### A. Dependence of the decoherence dynamics on the bath's chaoticity

An obvious difference between the chaotic and the regular baths emerges already at short times. For  $J \gg b$ ,  $\rho_{12}$  exhibits slowly decaying oscillations with the frequency of order of  $J$ , which mirror the quantum oscillations of the central system between the singlet and triplet states. The decay of the  $\rho_{12}$  oscillations is caused by the system's decoherence, and therefore directly monitors the dynamics of the decoherence process. We compare the oscillations decay for chaotic vs regular baths by varying the intrabath coupling parameter  $\Gamma_0$ ; see Eq. (2). The onset of chaos in the bath, which happens at  $\Gamma_0 > \Gamma_{cr}$  is verified by calculating the level spacing statistics  $P(s)$  [7].  $P(s)$  agrees with the orthogonal Wigner-Dyson distribution for a chaotic bath and with the Poisson distribution for a regular bath. We also check that the large-scale spectral properties of the bath change weakly when the bath's dynamics changes from regular ( $\Gamma_0 < \Gamma_{cr}$ ) to chaotic ( $\Gamma_0 > \Gamma_{cr}$ ).

Figure 5 clearly shows, for moderate system-bath cou-

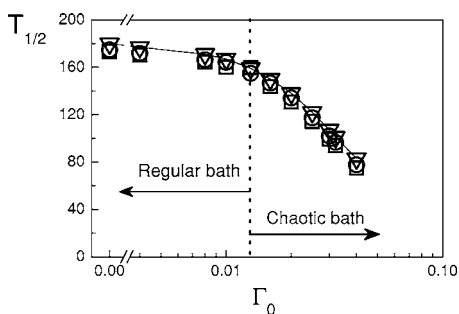


FIG. 6. Half-life time  $T_{1/2}$  for the decay of the reduced density matrix off-diagonal element  $\rho_{12}$  ( $\square$ ), system's linear entropy  $\Omega(t)$  ( $\nabla$ ), and fidelity of the central system  $F(t)$  ( $\circ$ ), as a function of  $\Gamma_0$ . The local magnetic field parameter is  $h_0=0.014$  and the central system–bath coupling is  $b=0.0683$ .

pling  $b$  (see below for details), that the decay of these oscillations strongly depends on the bath's chaoticity. Figure 5(a) shows the oscillations decay for two baths: one, with  $\Gamma_0=0.04 > \Gamma_{cr} \approx 0.013$ , is chaotic (solid line), and the other, with  $\Gamma_0=0.008 < \Gamma_{cr} \approx 0.013$ , is regular (dashed line). The difference in both the form and the rate of decay is obvious. The oscillation envelope  $\rho_{12}^{env}$  for the regular bath is fitted well by the Gaussian decay with the form

$$\rho_{12}^{env} = \alpha + \beta \exp(-t^2/T_s^2), \quad (7)$$

where  $T_s$  is the decay time,  $\alpha$  and  $\beta$  are constants. For the chaotic bath, the decay of oscillations is exponential, and is well fitted as

$$\rho_{12}^{env} = \alpha' + \beta' \exp(-t/T_s) \quad (8)$$

with the decay time  $T_s$  and constants  $\alpha'$  and  $\beta'$ . The transition of the form of decay from Gaussian to exponential is gradual, but strongly correlated with the transition of the bath's dynamics from regular to chaotic, as evident in Fig. 5(b). In order to demonstrate the form of decay more explicitly, only the envelopes  $\rho_{12}^{env}$  are shown in Fig. 5(b), without the high-frequency oscillations inside. Several envelopes are presented, which correspond to  $\Gamma_0$  gradually varying from zero to 0.04. It is clearly seen that for  $\Gamma_0 < \Gamma_{cr} \approx 0.013$  the envelopes do not change: the four solid curves obtained with  $\Gamma_0=0, 0.004, 0.008, 0.01$  practically coincide with each other. Thus, as long as the bath is regular, the decay is not affected by the value of  $\Gamma_0$ . But as soon as  $\Gamma_0$  crosses the value  $\Gamma_{cr}$ , and the bath becomes more and more chaotic, the changes become apparent: the curves for  $\Gamma_0=0.02$  (dashed),  $0.04$  (dotted), and  $0.08$  (dash-dotted) are clearly distinct, and the shape of decay varies from Gaussian to exponential. We emphasize that except for varying  $\Gamma_0$ , all other parameters of the Hamiltonian (1),(2) are kept constant.

The same behavior is demonstrated by the decay rate. Figure 6 shows the ‘‘half-life’’  $T_{1/2}$  of the oscillations as a function of  $\Gamma_0$ .  $T_{1/2}$  is the time at which the  $\rho_{12}$  oscillations reach half of their initial amplitude; the value  $T_{1/2}$  is determined without any assumptions about the form of  $\rho_{12}^{env}$  and therefore serves as a direct measure of the decay rate. For  $0 < \Gamma_0 < \Gamma_{cr} \approx 0.013$ , i.e., for regular baths, the half-life time

$T_{1/2}$  is not sensitive to the increase in the intrabath coupling  $\Gamma_0$ : the total variation of  $T_{1/2}$  from  $\Gamma_0=0$  to  $\Gamma_0=0.013$  is only 8%. A drastic change occurs as the dynamics of the bath becomes chaotic. For  $\Gamma_0 > \Gamma_{cr}$  the half-life time rapidly decreases with the increase of  $\Gamma_0$ . In the parameter interval  $0.013 < \Gamma_0 < 0.04$  the value of  $T_{1/2}$  decreases more than twice. Figure 6 clearly shows that the onset of chaos in the bath sharply changes the dependence of  $T_{1/2}$  on  $\Gamma_0$ . The chaotic bath leads to significantly faster decoherence, and the more chaotic is the bath the faster is the decoherence.

Note that this conclusion does not depend on which quantities we monitor. For example, the central system's linear entropy  $\Omega$  also shows decaying oscillations at short times, which are analogous to the  $\rho_{12}$  oscillations. The envelope of  $\Omega$  oscillations shows Gaussian decay for the regular bath, and exponential decay for the chaotic bath, similar to the  $\rho_{12}^{env}$  decay. The decay of  $\Omega$  oscillations can be quantified by the half-life time  $T_{1/2}$ , and Fig. 6 shows that both the  $\Omega$  oscillations and  $\rho_{12}$  oscillations have almost identical half-life time  $T_{1/2}$ . In a similar way, we can measure the central system decoherence by its fidelity  $F(t)$ . Fidelity measures the sensitivity of the central system to perturbations (in our case, to the impact of the bath), and is therefore analogous to the Loschmidt echo  $O(t)$ , see Eq. (5), which measures the sensitivity of the bath to perturbations.  $F(t)$  is defined by comparing the actual evolution of the central system, described by the density matrix  $\rho(t)$ , with the ideal evolution, described by the density matrix  $\rho'(t)$ , which would take place if the system and the bath did not interact,

$$F(t) = \text{Tr}_S[\rho'(t)\rho(t)], \quad (9)$$

where  $\text{Tr}_S$  denotes the trace over the states of the central system. The actual density matrix  $\rho$  of the central system is defined as  $\rho(t) = \text{Tr}_B \exp(-iHt) |\Psi(0)\rangle \langle \Psi(0)| \exp(iHt)$  where  $|\Psi(0)\rangle$  is the initial wavefunction of the compound system and  $H$  is given by Eq. (1), and the ideal density matrix  $\rho'$  is defined as  $\rho'(t) = \text{Tr}_B \exp(-iH't) |\Psi(0)\rangle \langle \Psi(0)| \exp(iH't)$ , where  $H' = JS_1 \cdot S_2 + H_B$  is the Hamiltonian corresponding to the ideal evolution of the central system decoupled from the bath. The short-time evolution of  $F(t)$  is similar to  $\rho_{12}$  and  $\Omega$ . The half-life time  $T_{1/2}$  of the  $F(t)$  oscillations is also presented in Fig. 6, and is very close to  $T_{1/2}$  obtained from  $\rho_{12}^{env}$  and  $\Omega$  decays.

### B. Dependence of the decoherence dynamics on the system-bath coupling and comparison with the Loschmidt echo decay

As we mentioned earlier, in our model the central system can not be treated as a perturbation:  $S_1$  cannot be replaced by a fictitious magnetic field since the intra-system and the system-bath couplings are isotropic. Also, our bath has no semiclassical limit. Nonetheless, there is a striking analogy between our results and the Loschmidt echo decay in semiclassical systems [10], which suggests that our results originate from generic properties of chaotic systems. To demonstrate the analogy, we study how the decoherence dynamics depends on the system-bath coupling  $b$ .

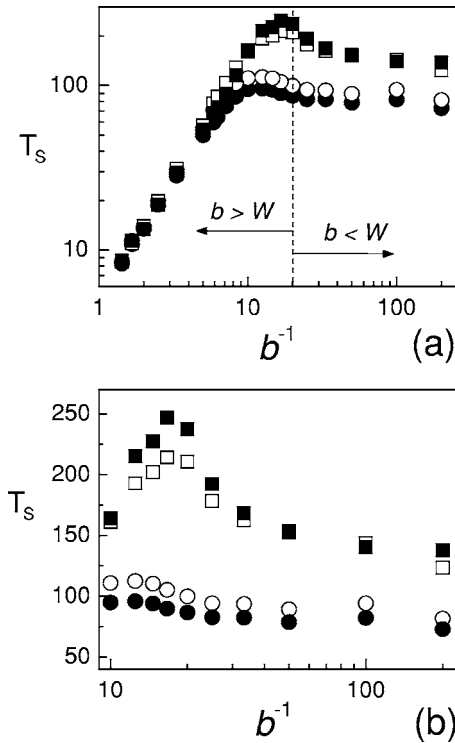


FIG. 7. Decoherence time  $T_s$  as a function of  $1/b$  for a chaotic bath with  $\Gamma_0=0.04$ ,  $h_0=0.014$  (circles), and for a regular bath with  $\Gamma_0=0.008$ ,  $h_0=0.014$  (squares). The values of  $T_s$  were obtained from the least-square fits of the decay of  $\rho_{12}^{\text{env}}$  to Gaussian (empty symbols) and exponential (solid symbols) forms. Figure (b) presents the same information as (a), but in semilogarithmic scale, in the restricted region of  $0.005 < b < 0.1$ .

For moderately small  $b$  the difference between the decoherence by the chaotic and by the regular bath is significant, see above. However, when  $b$  becomes comparable with the bath's spectral width  $W \approx 0.05$ , the difference becomes less pronounced, and for  $b > W$  the oscillations of  $\rho_{12}$  become identical for chaotic and for regular baths. To demonstrate how this happens, we present here the decay of  $\rho_{12}$  oscillations for two baths, one regular with  $\Gamma_0=0.008$ , and the other chaotic with  $\Gamma_0=0.04$ . The envelopes  $\rho_{12}^{\text{env}}$  obtained from simulations were fitted to both Gaussian (7) and exponential (8) form; the values of  $T_s$  obtained from the least-square fits to the Gaussian and to the exponential forms are close to each other. The resulting decay times  $T_s$  are presented in Fig. 7(a) as a function of  $1/b$  in log-log scale. The difference between the chaotic and the regular bath is clearly seen for  $b < W$ , the corresponding decoherence times differ by a factor of 2–2.5, in agreement with the conclusion that the chaotic bath leads to faster decoherence. At  $b > W$  the difference becomes smaller, and quickly disappears with increasing  $b$  (decreasing  $1/b$ ); at  $b \gg W$ ,  $T_s$  is almost inversely proportional to  $b$  for both baths. Also, at  $b < W$  the behavior of  $T_s(1/b)$  is different for the chaotic and for the regular bath, see the inset in Fig. 7(b) which presents  $T_s$  in linear scale. In the region  $0.005 < b < 0.05$ , the decoherence time in the case of the regular bath changes by about a factor of 2 [22]. In contrast, for the chaotic bath  $T_s$  remains almost constant: the total variation of  $T_s$  is less than 15% in the same region of  $b$ .

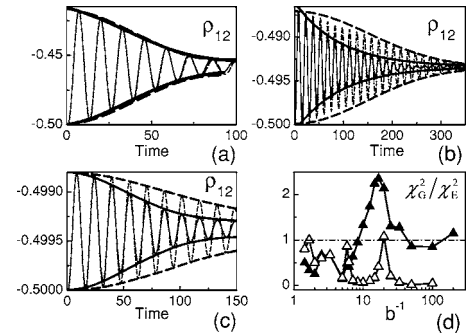


FIG. 8. Short-time evolution of the off-diagonal element  $\rho_{12}$  in the case of a chaotic environment  $\Gamma_0=0.04$ ,  $h_0=0.014$  (solid curves) and in the case of a nonchaotic environment  $\Gamma_0=0.008$ ,  $h_0=0.014$  (dashed curves). The coupling between the two central spins is  $J=0.4$ . The values of the interaction between the central system and its environment are  $b=0.2$  (a),  $b=0.0683$  (b), and  $b=0.02$  (c). For  $b=0.2$  (a), the oscillations for the chaotic and the regular bath are almost identical, so that the solid and the dashed curves nearly coincide. We keep a spectrum bandwidth of  $W \approx 0.05$  for the two baths. Panel (d) presents the ratio  $\chi_G^2/\chi_E^2$  as a function of  $1/b$  in case of the chaotic bath ( $\blacktriangle$ ) and in case of the regular bath ( $\triangle$ ).

Note that all the regimes seen in Fig. 7 do not depend on the quantity we monitor, and the linear entropy  $\Omega(t)$  and the fidelity  $F(t)$  demonstrate the same behavior as the matrix element  $\rho_{12}(t)$ .

On a heuristic level, we can draw an analogy with the LE decay, identifying the central system's states  $|\uparrow\downarrow\rangle$  and  $|\downarrow\uparrow\rangle$  with the states  $|q_1\rangle$  and  $|q_2\rangle$  of Sec. I, and the strength of the system-bath interaction  $b$  with the strength of the perturbation  $V$ . The behavior of  $T_s$  as a function of  $b$  then exhibits clear similarities with the LE decay. For strong perturbations, the LE decay is Gaussian, and the rate is the same for the chaotic and for the regular bath. This is similar to  $T_s$  for  $b \gg W$ . As the strength of the perturbation decreases, the chaotic bath enters the Lyapunov's regime, where LE decay is exponential with the rate independent of the perturbation, while the LE decay for the regular bath remains Gaussian with the decay time which is smaller than the decay time for the chaotic system. This is very similar to the behavior of  $T_s$  in the region  $b < W$ . With further decrease of  $b$ , we would expect to enter the perturbative regime of decoherence, but for  $b < 0.005$  the oscillations of  $\rho_{12}$  have too small an amplitude to make the studies sufficiently conclusive.

The form of the decay of  $\rho_{12}$  oscillations is also similar to the form predicted for the LE decay, although agreement is not as good as for the decay time  $T_s$ . This is due to the fact that the initial decay is always Gaussian, and the exponential decay, if it exists, sets in at later times. To quantify the form of decay of  $\rho_{12}$  oscillations, we fit  $\rho_{12}^{\text{env}}$  for chaotic and regular baths to both Gaussian and exponential form, and for every fit calculate the  $\chi^2$  deviation. The examples of  $\rho_{12}$  oscillations and the fittings are given in Figs. 8(a)–8(c), and the dependence of  $\chi^2$  on  $1/b$  for the chaotic and the regular bath is presented in Fig. 8(d). The value of  $\chi_E^2$  (respectively,  $\chi_G^2$ ) measures the mean distance between the calculated  $\rho_{12}^{\text{env}}$  envelope and the closest exponential (respectively Gaussian) curve fitting the envelope. For decoherence by the regular



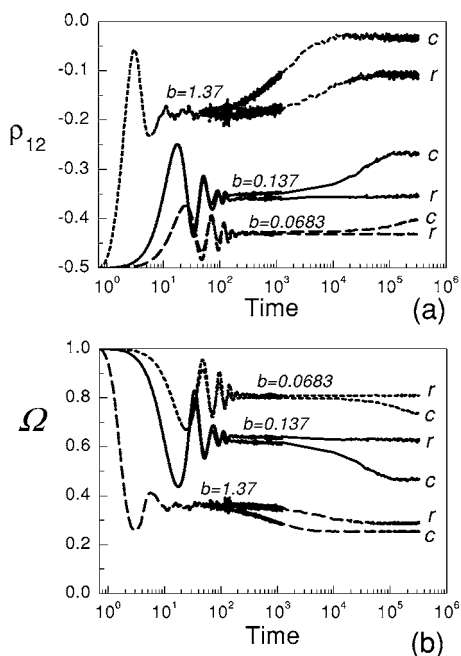


FIG. 9. Global time evolution of (a) the off-diagonal element  $\rho_{12}(t)$  and (b) the central system's linear entropy  $\Omega$  in the case of a chaotic bath  $\Gamma_0=0.04$ ,  $h_0=0.014$  (the curves marked as *c*) and in the case of a regular bath  $\Gamma_0=0.008$ ,  $h_0=0.014$  (the curves marked as *r*). The coupling between the central spins is  $J=0.1$ . The values of the coupling between the central system and its bath are  $b=0.0683$ ,  $b=0.137$ , and  $b=1.37$ .

bath, the  $\rho_{12}^{\text{env}}$  decay is Gaussian almost everywhere: in the whole range of couplings  $0.005 < b < 1.37$  for the regular bath  $\chi_G^2 \ll \chi_E^2$  except for few values of  $b$  near  $b \sim W$  where  $\chi_G^2 \approx \chi_E^2$ . For the case of decoherence by the chaotic bath in the region  $b < W$ , when the LE decay is exponential (Lyapunov's regime), the decay of  $\rho_{12}$  oscillations is also exponential (with  $\chi_E^2$  noticeably smaller than  $\chi_G^2$ ), or, at least, shows a tendency to be exponential, with  $\chi_G^2 \approx \chi_E^2$ .

Thus, an interesting question arises, whether the chaotic bath at  $b < W$  is in Lyapunov's regime. Our data agree with this conclusion ( $T_s$  is only weakly dependent on the value of  $b$ , and the decay of  $\rho_{12}$  oscillations is close to exponential), but more detailed studies are needed in order to prove that conjecture. Since the notion of a wavepacket and its trajectory is not applicable to the bath of many spins  $1/2$ , it would be very interesting to understand the physical meaning of the Lyapunov's regime and Lyapunov's exponents [23].

It may also be interesting to establish the connection between our numerical results and the experimental results of Ref. [24]. However, in order to make such a connection scientifically sound, more work is still required.

#### IV. LONG-TIME EVOLUTION OF THE CENTRAL SYSTEM AND THE POINTER STATES

##### A. Long-time decoherence of the central system

The long-time evolution of the central system also demonstrates pronounced differences between the decoherence

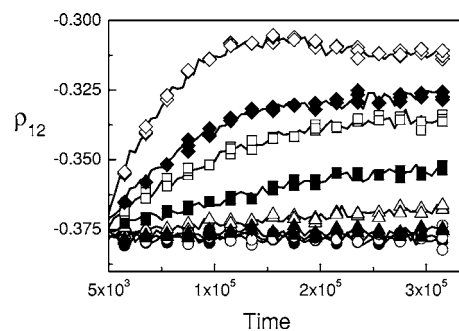


FIG. 10. Long-time evolution of the off-diagonal element  $\rho_{12}$  for a central system-bath coupling  $b=0.114$ , in the case of regular baths ( $\bullet$ )  $\Gamma_0=0$ , ( $\circ$ )  $\Gamma_0=0.008$ , and ( $\blacktriangle$ )  $\Gamma_0=0.013$ , and in the case of chaotic baths ( $\triangle$ )  $\Gamma_0=0.02$ , ( $\blacksquare$ )  $\Gamma_0=0.025$ , ( $\square$ )  $\Gamma_0=0.03$ , ( $\blacklozenge$ )  $\Gamma_0=0.032$ , and ( $\diamond$ )  $\Gamma_0=0.04$ . For all the baths, the local magnetic field parameter is  $h_0=0.014$ . The coupling between the two central spins is  $J=0.1$ .

by chaotic and by regular baths. Figure 9 shows the long-time evolution of the reduced density matrix off-diagonal element  $\rho_{12}$  [Fig. 9(a)] and of the central system's linear entropy  $\Omega$  [Fig. 9(b)] for different system-bath couplings  $b$ . For every value of  $b$  two curves are shown, corresponding to a chaotic bath  $\Gamma_0=0.04 > \Gamma_{cr}$  (marked as "c") and to a regular bath  $\Gamma_0=0.008 < \Gamma_{cr}$  (marked as "r"). In Fig. 9(a) we see that the chaotic bath, for a fixed value of  $b$ , is more efficient in steering the pointer-state value  $\rho_{12}^{\text{pt}}$  of  $\rho_{12}$  towards zero, i.e., in breaking the entanglement between the two central spins. Figure 9(b) confirms this observation: the central system linear entropy  $\Omega$  is more efficiently steered towards the limit  $1/4$  (which corresponds to a maximally mixed central system) in the presence of a chaotic bath.

It is important to note that in the case of decoherence by a chaotic bath, even for very weak coupling  $b$ , both stages of the decoherence process are always present, and the system exhibits both initial decay of oscillations and the long-term relaxation of  $\rho_{12}$  and  $\Omega$  to their pointer-state values. In contrast, for the regular bath, the second stage is usually absent; after the decay of the short-time oscillations the values of  $\rho_{12}$  and  $\Omega$  stay constant (see the curves for  $b=0.0683$ ,  $0.137$  in Fig. 9). Only for very strong system-bath coupling  $b > J > W$  does the regular bath induce a long-time decoherence in the central system (see curves  $b=1.37$  in Fig. 9). In order to demonstrate that the onset of chaos is responsible for the second stage of the decoherence process, we have calculated the long-time evolution of  $\rho_{12}$  for a fixed value of  $b=0.114$  and for different chaotic and regular baths. Figure 10 clearly shows that no long-time decoherence process is induced as long as  $\Gamma_0 < \Gamma_{cr}$ , i.e., as long as the bath is not chaotic. However, once  $\Gamma_0$  crosses the value  $\Gamma_{cr}$ , the long-term decoherence is clearly seen, and the pointer-state value  $\rho_{12}^{\text{pt}}$  becomes closer to zero with increasing  $\Gamma_0$ .

This behavior is exactly what we have observed in studying the dependence of the short-time decoherence on  $\Gamma_0$ : no changes in the form or the time of decay are observed for  $\Gamma_0 < \Gamma_{cr}$ , but as soon as  $\Gamma_0$  exceeds  $\Gamma_{cr}$ , the decay form and the decay time start to change rapidly.



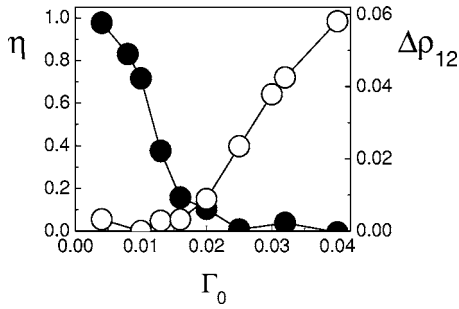


FIG. 11. Left axis: Parameter  $\eta$  (●), measuring the chaoticity of the bath, as a function of  $\Gamma_0$ , for  $h_0=0.014$ , as a function of  $\Gamma_0$ . Right axis: Variation  $\Delta\rho_{12}$  (○) of the element  $\rho_{12}$  in the time interval  $5 \times 10^3 < t < 3.2 \times 10^5$  for  $b=0.114$  and  $J=0.1$ , as a function of  $\Gamma_0$ . The two curves exhibit clear correlation with each other.

For more detailed study, we quantify the chaoticity of the bath by the statistics of the level splittings  $P(s)$ , using the parameter

$$\eta = \frac{\int_0^{s_0} (P(s) - P_{\text{WD}}(s)) ds}{\int_0^{s_0} (P_p(s) - P_{\text{WD}}(s)) ds}, \quad (10)$$

where  $P_p(s) = \exp(-s)$  is the Poisson distribution characteristic for regular baths, and  $P_{\text{WD}}(s) = (\pi s/2) \exp(-\pi s^2/4)$  is the orthogonal Wigner-Dyson distribution characterizing the chaotic baths. The quantity  $\eta$  is a standard measure of the chaoticity [18,25]. The abscissa  $s_0 \approx 0.4729$  determines the first intersection point of the two distributions,  $P_p(s_0) = P_{\text{WD}}(s_0)$ . The value of  $\eta=0$  means that the bath is chaotic and  $P(s) = P_{\text{WD}}(s)$ , while  $\eta=1$  means that the bath is regular with  $P(s) = P_p(s)$ . In Fig. 11, we present the parameter  $\eta$  as a function of  $\Gamma_0$ . In the same graph, we plot the long-time variation of  $\rho_{12}$  in the time interval  $5 \times 10^3 < t < 3.2 \times 10^5$ , denoted as  $\Delta\rho_{12}$ . The correlation between the two graphs is clear. The regular-to-chaotic transition occurs around  $\Gamma_{\text{cr}} \sim 0.013$ , and for  $\Gamma_0 < \Gamma_{\text{cr}}$  the value of  $\Delta\rho_{12}$  remains very small, less than 0.003, while between  $\Gamma_0 = \Gamma_{\text{cr}}$  and  $\Gamma_0 \approx 3\Gamma_{\text{cr}}$  the value of  $\Delta\rho_{12}$  changes by a factor of 30. This clearly shows that the onset of chaos in the bath induces drastic changes in the long-time decoherence of the central system.

### B. Impact of the chaoticity of the bath on the pointer states of the central system

Finally, we study the impact of chaos in the bath on the pointer states of the central system, by considering how the curve  $\rho_{12}^{\text{pt}}(J/b)$  changes with variation of the bath's parameters. Figure 12 presents the curves  $\rho_{12}^{\text{pt}}(J/b)$  for different baths with different values of  $\Gamma_0$  and  $h_0$ ; note that  $\Gamma_0$  and  $h_0$  vary by an order of magnitude from one curve to another. For a fixed value of the ratio  $J/b$ , the increase of the local magnetic field  $h_0$  leads to a decrease of  $|\rho_{12}^{\text{pt}}|$ . The same happens with the increase of the intrabath coupling  $\Gamma_0$ . Increas-

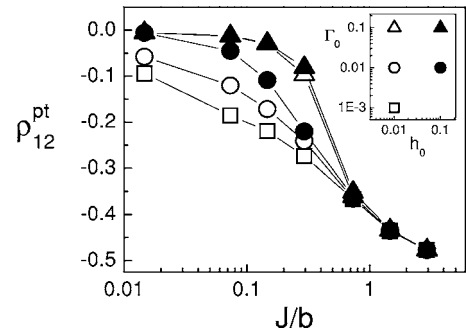


FIG. 12. Pointer state value  $\rho_{12}^{\text{pt}}$  of the off-diagonal matrix element  $\rho_{12}$  as a function of the ratio  $J/b$  for different parameters  $\Gamma_0$  and  $h_0$  of the bath:  $\Gamma_0=0.1$ ,  $h_0=0.1$  (▲),  $\Gamma_0=0.1$ ,  $h_0=0.01$  (△),  $\Gamma_0=0.01$ ,  $h_0=0.1$  (●),  $\Gamma_0=0.01$ ,  $h_0=0.01$  (○),  $\Gamma_0=0.001$ , and  $h_0=0.01$  (□). The curves corresponding to  $\Gamma_0=0.1$ ,  $h_0=0.1$  (▲), and  $\Gamma_0=0.1$ ,  $h_0=0.01$  (△) almost coincide with each other. The values of  $\Gamma_0$  and  $h_0$  can also be read in the inset (note the log-log scale used there).

ing  $\Gamma_0$  or  $h_0$  makes the bath's internal dynamics faster, so that the main trend demonstrated by Fig. 12 is that the faster the bath's internal dynamics the stronger is decoherence. However, the onset of chaos also influences the pointer states, although not so drastically. For example, comparison between the curves  $\Gamma_0=0.01$ ,  $h_0=0.1$  (●), and  $\Gamma_0=0.1$ ,  $h_0=0.01$  (△) shows that the increase in  $\Gamma_0$ , which makes the bath more chaotic, leads to much bigger changes of the curve  $\rho_{12}^{\text{pt}}(J/b)$  than the increase in  $h_0$  which makes the bath faster but less chaotic. The chaotic bath, for the same value of  $J/b$ , is more efficient in steering  $\rho_{12}^{\text{pt}}$  towards zero, i.e., in breaking the correlations between  $\mathbf{S}_1$  and  $\mathbf{S}_2$ .

## V. CONCLUSIONS

We have studied decoherence of a two-spin system by regular and chaotic spin baths. We go beyond the standard one-body semiclassical description, considering environments of many spins 1/2. We do not replace the system or the bath by a perturbation, thus going beyond the Loschmidt echo (LE) studies, and consider situations where the LE-type arguments are not applicable. As  $t \rightarrow \infty$ , the chaotic bath leads to smaller values of the system's density matrix element  $\langle \uparrow \downarrow | \rho | \downarrow \uparrow \rangle$ , and to smaller values of the central system's entropy than the regular bath, i.e., at long times the chaotic bath decoheres the system more efficiently. At short times, the chaotic bath leads to faster decay of quantum oscillations in the system, and changes the form of the decay from Gaussian to exponential. Therefore, the onset of chaos in the bath drastically changes the decoherence dynamics, although the large-scale properties of the bath spectrum (such as the spectral width) are influenced very weakly. It is interesting that the conclusions based on qualitative semiclassical arguments agree, in general, with our calculations, although the bath of many spins 1/2 does not have a semiclassical single-spin analog. Based on the established analogy with the Loschmidt echo decay, we presented arguments that the chaotic bath is in the Lyapunov's dynamical regime.

## ACKNOWLEDGMENTS

The authors would like to thank D. Shepelyansky, B. Georgeot, P. Jacquod, W. Zurek, J.-P. Paz, L. Viola, F. Cucchietti, and M. Dzero for helpful discussions. This work was

supported by the National Security Agency (NSA) and Advanced Research and Development Activity (ARDA) under Army Research Office (ARO) contract DAAD 19-03-1-0132.

- 
- [1] J. von Neumann, *Mathematical Foundations of Quantum Mechanics* (Princeton University Press, Princeton, NJ, 1955); D. Giulini, E. Joos, C. Kiefer, J. Kupsch, I.-O. Stamatescu, and H. D. Zeh, *Decoherence and the Appearance of a Classical World in Quantum Theory* (Springer-Verlag, Berlin, Heidelberg, New York, 1996).
- [2] C. J. Myatt *et al.*, *Nature* (London) **403**, 269 (2000).
- [3] Yu. A. Pashkin *et al.*, *Nature* (London) **421**, 823 (2003).
- [4] H. J. Mamin, R. Budakian, B. W. Chui, and D. Rugar, *Phys. Rev. Lett.* **91**, 207604 (2003).
- [5] M. Nielsen and I. Chuang, *Quantum Computation and Quantum Information* (Cambridge University Press, Cambridge, UK, 2000).
- [6] C. W. Gardiner and P. Zoller, *Quantum Noise* (Springer-Verlag, Berlin, Heidelberg, New York, 2000).
- [7] F. Haake, *Signatures of Quantum Chaos* (Springer-Verlag, Berlin, Heidelberg, New York, 2001).
- [8] W. Zurek, *Nature* (London) **412**, 712 (2001).
- [9] R. Alicki, quant-ph/0205173; T. Prosen and M. Žnidarič, *J. Phys. A* **35**, 1455 (2002).
- [10] Ph. Jacquod, *Phys. Rev. Lett.* **92**, 150403 (2004); D. Poulin, R. Blume-Kohout, R. Laflamme, and H. Ollivier, *Phys. Rev. Lett.* **92**, 177906 (2004); T. Prosen and M. Žnidarič, *J. Phys. A* **36**, 2463 (2003); D. A. Wisniacki, *Phys. Rev. E* **67**, 016205 (2003); Ph. Jacquod, I. Adagideli, and C. W. J. Beenakker, *Phys. Rev. Lett.* **89**, 154103 (2002); N. R. Cerruti and S. Tomsovic, *Phys. Rev. Lett.* **88**, 054103 (2002); W. Wang and B. Li, *Phys. Rev. E* **66**, 056208 (2002); F. M. Cucchietti, C. H. Lewenkopf, E. R. Mucciolo, H. M. Pastawski, and R. O. Vallejos, *Phys. Rev. E* **65**, 046209 (2002); Z. P. Karkuszewski, C. Jarzynski, and W. H. Zurek, *Phys. Rev. Lett.* **89**, 170405 (2002); A. Jordan and M. Srednicki, quant-ph/0112139; R. A. Jalabert and H. M. Pastawski, *Phys. Rev. Lett.* **86**, 2490 (2001); Ph. Jacquod, P. G. Silvestrov, and C. W. J. Beenakker, *Phys. Rev. E* **64**, 055203(R) (2001).
- [11] J. Emerson, Y. S. Weinstein, S. Lloyd, and D. G. Cory, *Phys. Rev. Lett.* **89**, 284102 (2002).
- [12] R. de Sousa and S. Das Sarma, *Phys. Rev. B* **68**, 115322 (2003); **67**, 033301 (2003).
- [13] A. Garg, *Phys. Rev. Lett.* **74**, 1458 (1995); N. V. Prokof'ev and P. C. E. Stamp, *Rep. Prog. Phys.* **63**, 669 (2000).
- [14] R. Vrijen, E. Yablonovitch, K. Wang, H. W. Jiang, A. Balandin, V. Roychowdhury, T. Mor, and D. DiVincenzo, *Phys. Rev. A* **62**, 012306 (2000).
- [15] R. W. Simmonds *et al.*, cond-mat/0402470.
- [16] A. Abragam, *The Principles of Nuclear Magnetism* (Clarendon Press, Oxford, 1961).
- [17] M. I. Katsnelson, V. V. Dobrovitski, H. A. De Raedt, and B. N. Harmon, *Phys. Lett. A* **318**, 445 (2003).
- [18] B. Georgeot and D. L. Shepelyansky, *Phys. Rev. Lett.* **81**, 5129 (1998).
- [19] V. V. Dobrovitski and H. A. De Raedt, *Phys. Rev. E* **67**, 056702 (2003).
- [20] H. De Raedt and V. V. Dobrovitski, in *Computer Simulation Studies in Condensed-Matter Physics XVI*, edited by D. P. Landau, S. P. Lewis, and H.-B. Schüttler (Springer-Verlag, Berlin, Heidelberg, New York, 2004).
- [21] J. P. Paz and W. H. Zurek, *Phys. Rev. Lett.* **82**, 5181 (1999).
- [22] It is interesting that at  $0.01 < b < 0.1$ , for the regular bath,  $T_S$  decreases by a factor of  $\sim 2$  with decreasing  $b$ , i.e., the system is decohered faster for smaller system-bath interaction, while for the chaotic bath  $T_S$  is almost constant (the change is  $\sim 13\%$ ). This effect is supported by other simulations, but the simple explanation is yet to be found.
- [23] V. V. Flambaum and F. M. Izrailev, *Phys. Rev. E* **64**, 036220 (2001); **64**, 026124 (2001).
- [24] H. M. Pastawski, P. R. Levstein, G. Usaj, J. Raya, and J. Hirschinger, *Physica A* **283**, 166 (2000).
- [25] B. Georgeot and D. L. Shepelyansky, *Phys. Rev. E* **62**, 6366 (2000).